A 24-GHz Low-cost Continuous Beam Steering Phased Array for Indoor Smart Radar

Zhengyu Peng[1], Lixin Ran[2], and Changzhi Li[1], *Senior Member, IEEE*
[1]Depart. of Electrical & Computer Engineering, Texas Tech University, Lubbock, TX 79409, USA
[2]Depart. of Information and Electronic Engineering, Zhejiang University, Hangzhou, 310027, China
Email: zhengyu.peng@ttu.edu, ranlx@zju.edu.cn, changzhi.li@ttu.edu

***Abstract*—A 24-GHz phased array for indoor smart radar is proposed in this paper. This array consists of 6 horizontally placed antenna elements. Each antenna element is a vertically placed 5-element series-fed microstrip patch array. The beam of the phased array can be continuously steered on the H-plane to different directions through a novel vector control array. Each element of the vector control array can adjust the phase and amplitude of the corresponding element of the horizontally placed linear array. The whole phased array system is fabricated on a single printed circuit board (PCB). PIN diodes are used to realize beam steering by modulating the decomposed received signal. In order to compensate for the loss of the vector control array and reduce the noise figure, six low noise amplifiers (LNAs) are also used in the array. This proposed phased array system features a lower cost than conventional solutions based on phase shifters. The principle of the proposed vector control array is discussed, and simulation shows this system has the ability to continuously steer the beam on the H-plane.**

***Index Terms*—Beam steering, phased array, vector control array, radar.**

I. Introduction

FOR nearly a century, radar system has been used for imaging, ranging and detection in navigation, space and military applications. Because of the advancement of semiconductor technology and design methodology, in recent years, applications of radar systems have been expended to commercial areas, such as automobile [1], industrial localization [2], and biomedical applications [3]. In many cases, the radar system scans the objects line-by-line or sector-by-sector with a mechanical steering antenna or array. Usually the mechanical steering system will increase the size, weight, and cost. It may also limit the reliability of the entire system. With the heavy and bulky mechanical system, it is difficult to mount the radar on an automobile or medical equipment. One example that needs modern low-profile radar with beam steering capability is tumor tracking for lung cancer radiotherapy, where it is desirable for the biomedical radar mounted on a medical linear accelerator (LINAC) to dynamically steer the beam between the chest and abdomen of the patient to monitor the respiration pattern and track tumor location during radiation therapy [4].

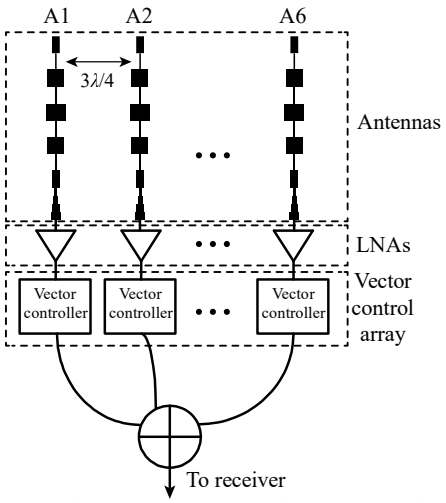

Fig. 1. Schematic of the proposed continuous beam steering phased array.

Phased-array radar overcomes the drawbacks of mechanical beam steering system. With electrical beam steering, the radar system can scan a wide sector in milliseconds [5]. Since it is easy to implement phased array radar system on a printed circuit board (PCB), it will have a much lighter weight and lower profile, which enable the radar to be mounted on an automobile without affecting the outline or structure of the automobile. With lighter weight and lower profile, the radar is also much easier to be implemented on medical equipment and installed at home for smart house applications. However, the conventional phased array is expensive, especially at frequencies higher than 24 GHz. This is mainly because conventional solutions require high frequency phase shifters, which are expensive and have a small number of manufacturers.

In this paper, a 24-GHz horizontally placed 6-element phased array is designed for portable smart radar receivers. The beam on the H-plane can be continuously tuned to different directions using a vector control array. Moreover, with the ability of independently adjusting the phase and amplitude of each antenna element, the proposed phased array can also realize more complex beam forming. Due to the elimination of the requirement of phase shifters, the cost of the proposed system is significantly reduced from a conventional phased array. The principle of the antenna array and vector control array will be discussed in Section II, and simulation results will be presented in Section III. A discussion and conclusion will be drawn in Section IV.

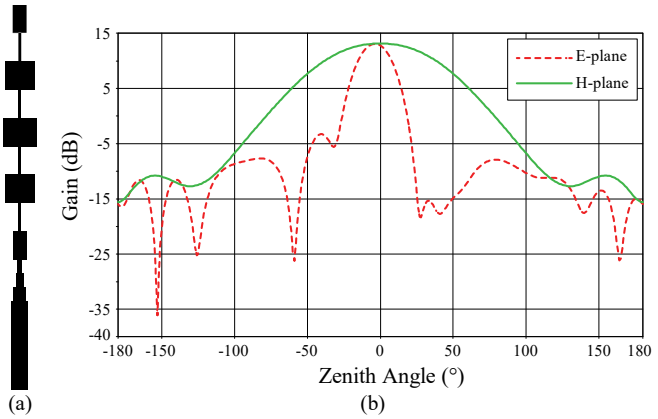

Fig. 2. (a) Series-fed Dolph-Chebychev distributed array. (b) The E-plane and H-plane patterns of the series-fed Dolph-Chebychev distributed array.

II. Theory and Design

Figure 1 shows the block diagram of the proposed continuous beam steering phased array. In the first stage, the antenna array is designed to obtain a narrow beamwidth and low sidelobe on the E-plane and to be steerable on the H-plane. This means the array can scan along the horizontal plane. Beam steering is achieved by a vector control array. Each vector controller in the vector control array can independently adjust the phase and amplitude of the signal from one of the antenna elements. The vector control array is designed on the PCB with PIN diodes, which results in a low system cost and a low profile. In order to compensate for the insertion loss of the vector control array and improve the sensitivity of the receiver system, a low noise amplifier (LNA) is added between each antenna element and its corresponding vector controller.

A. Antenna Array

The design of the antenna array aims to create a non-steerable, narrow beamwidth on the E-plane (i.e., along the vertical direction) and a steerable pattern on the H-plane (i.e., along the horizontal direction), such that the radar system can perform 1-D electrical scan by adjusting the vector control array.

Fig. 2(a) shows one array element, which consists of five series-fed microstrip patch antennas with Dolph-Chebychev distribution, which has the minimum null-to-null beamwidth for a specified sidelobe level and equal magnitude for all the sidelobes [6]. Fig. 2(b) shows the radiation pattern of one array element. The E-plane pattern has a narrow beam directing to 0°, and the H-plane pattern has a wide beam. In this phased array, 6 series-fed patch arrays are distributed horizontally, the distance between each element is $3\lambda/4$. By feeding these 6 antenna elements with different phases and amplitudes, continuous beam steering can be realized.

B. Vector Controller

Assume a complex signal $x'=\exp(-j2\pi ft-j\Phi(t))$, where f is the frequency and $\Phi(t)$ is the modulation phase. By multiplying x with $w=R\exp(j\phi)$, the result y is the original signal x modulated

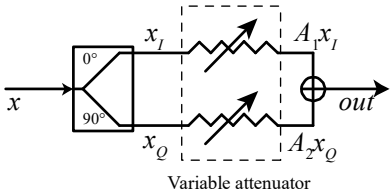

Fig. 3. Principle of the vector controller.

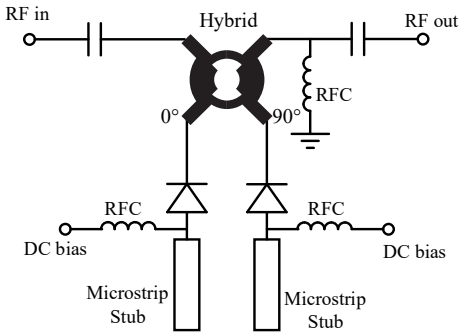

Fig. 4. Schematic of the reflection-type attenuator.

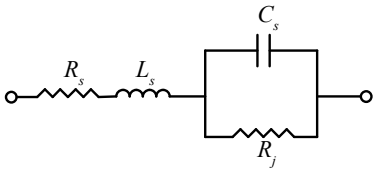

Fig. 5. Equivalent circuit model for the PIN diode.

by amplitude R and phase ϕ.

$$y = Re^{-j(2\pi ft+\emptyset(t)-\phi)} \tag{1}$$

The real part of y, which is the combination of the in-phase and quadrature components, is:

$$\begin{aligned} Re\{y\} &= R\cos(2\pi ft+\emptyset(t)-\phi) \\ &= R\cos\phi\cos(2\pi ft+\emptyset(t)) + R\sin\phi\sin(2\pi ft+\emptyset(t)) \end{aligned} \tag{2}$$

This suggests that amplitude and phase control can be easily realized through a vector controller shown in Fig. 3. The input signal x is divided into in-phase signal $x_I = \sin(2\pi ft+\emptyset(t))$ and quadrature signal $x_Q = \cos(2\pi ft+\emptyset(t))$ by a quadrature power divider. After passing through the variable attenuators, the in-phase signal is attenuated by $A_1 = R\cos\phi$ and the quadrature signal is attenuated by $A_2 = R\sin\phi$. After combing these two signals, the output of the vector controller will be the same as (2), realizing an amplitude change of R and a phase shift of ϕ to the input signal x.

C. Constant Phase Shift Variable Attenuator

As mentioned above, two attenuators are used in one vector controller. In order to realize the function of the vector controller, the phase shift of a single attenuator should be constant when the attenuation changes.

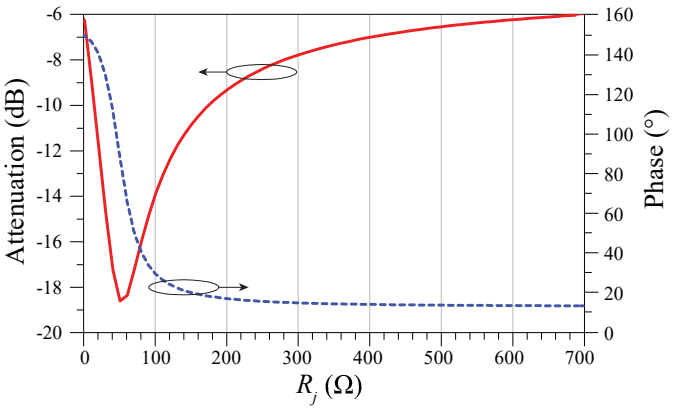

Fig. 6. Attenuation and phase of the attenuator according to the change of the intrinsic layer resistance at 24 GHz.

A constant-phase-shift variable attenuator is designed in this paper. Fig. 4 is the schematic of this attenuator, which is a reflection-type attenuator with good impedance matching at both the input and output because of its symmetric structure [7]. The two diodes used in this attenuator are PIN diodes.

A PIN diode obeys the standard diode equation for low-frequency signals. However, at higher frequencies, the diode can be modeled as a resistor R_j with some parasitic capacitance and inductance, as shown in Fig. 5 [8]. C_s, L_s, and R_s are parasitic capacitor, inductor and resistor respectively. R_j is the intrinsic layer resistance of PIN diode, the value of R_j can be controlled by DC bias current [9]. This is the key to realize a variable attenuator.

The operation of the reflection-type attenuator can be explained as follows. When $R_j \cong 50\Omega$, since the hybrid output ports are matched, all the RF signal is absorbed by the PIN diodes, and it is not transmitted to "RF out" at the isolation port of the hybrid. Thus, attenuation in this situation is the maximum. When decreasing the diode resistance to near 0 or increasing it to a very large value by changing the bias current, the RF signal will be completely reflected at the ports of the PIN diodes and transmitted to the "RF out" port. In this case, the attenuation is the minimum.

Since the PIN diode is not a perfect resistor at high frequencies, it has parasitic capacitor and inductor. The RF signal passes through the PIN diode will have different phase shifts with different R_j. If R_j is very small, it will short the parasitic capacitor, and the parasitic inductor will contribute to the phase shift. On the other hand, if R_j is very large, the parasitic capacitor will also contribute to the phase shift. However, for the reflection-type attenuator, the phase shift will be constant.

Fig. 6 shows the simulation result of the reflection-type attenuator at 24 GHz with different R_j and realistic parasitics. The attenuation is the maximum when R_j is about 50Ω, and the attenuation will decrease when the value of R_j is either increased or decreased from 50Ω. The phase is stable when R_j increases from 100Ω to 700Ω.

III. Simulation Results

The simulation of the phased array is performed on a commercial FDTD simulation tool. The different patterns of the array are simulated based on the different phase and amplitude values generated by the vector control array.

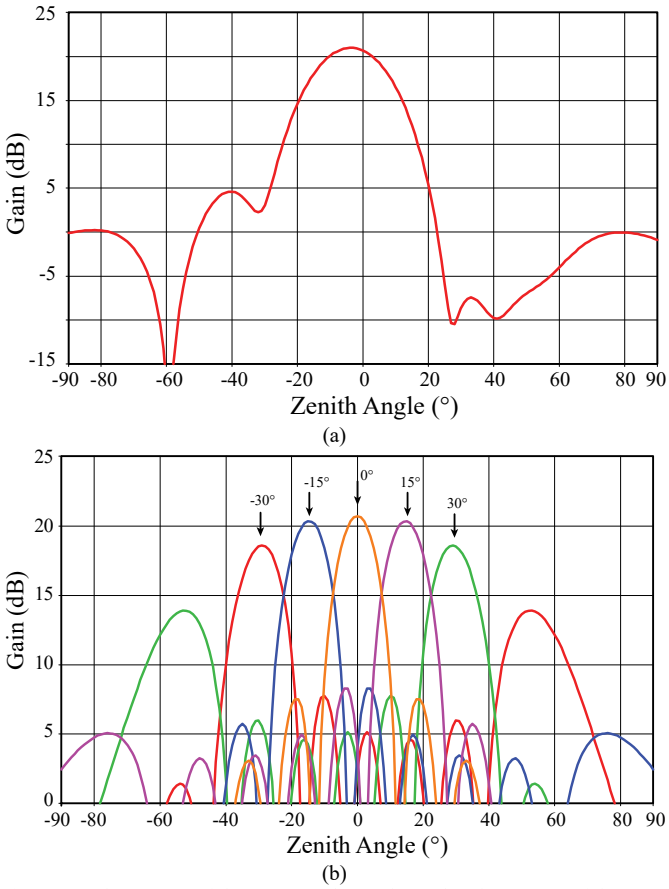

Fig. 7. (a) The pattern of the array on the E-plane. (b) The pattern of the array on the H-plane with beam direction tuning.

TABLE I. Phase and Amlitude Values to Achieve Fig. 7(b).

Direction		A1	A2	A3	A4	A5	A6
-30°	Phase	0°	135°	270°	45°	180°	315°
	Amplitude	1	1	1	1	1	1
-15°	Phase	0°	70°	140°	210°	280°	350°
	Amplitude	1	1	1	1	1	1
0°	Phase	0°	0°	0°	0°	0°	0°
	Amplitude	1	1	1	1	1	1
15°	Phase	350°	280°	210°	140°	70°	0°
	Amplitude	1	1	1	1	1	1
30°	Phase	315°	180°	45°	270°	135°	0°
	Amplitude	1	1	1	1	1	1

Fig. 7 shows the simulated patterns of the continuous beam steering phased array. Fig. 7(a) is the E-plane pattern of the phased array, which has a narrow beamwidth of 22.8°. Due to the Dolph-Chebychev distribution, the sidelobe level on the E-plane can reach to -16.4 dB. Fig. 7(b) is the H-plane pattern of the array. The main beam can be tuned to different directions by adjusting the phase differences of each antenna element through the vector control array. The direction of the beam can be tuned continuously since the phase of each vector controller can be adjusted continuously. Table I reports the phase and amplitude values to achieve Fig. 7(b) in simulation.

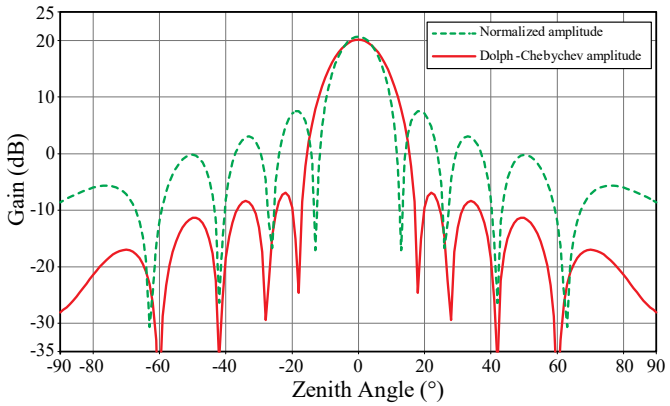

Fig. 8. The pattern of the array with normalized amplitude feed and the pattern of the array with Dolph-Chebychev amplitude feed.

TABLE II. PHASE AND AMPLITUDE VALUES TO ACHIEVE FIG. 8.

		A1	A2	A3	A4	A5	A6
Normalized	Phase	0°	0°	0°	0°	0°	0°
	Amplitude	1	1	1	1	1	1
Dolph-Chebychev	Phase	0°	0°	0°	0°	0°	0°
	Amplitude	0.36	0.72	1	1	0.72	0.36

In Fig. 7(b), the direction of the beam is tuned only by adjusting the phase of each antenna element. In this proposed array, the vector control array can not only change the phase of the each antenna element, but also adjust the amplitude of each antenna element. With independent phase and amplitude control, the array can be used to form more complex or more promising patterns in radar applications. Fig. 8 is one of the examples to form a pattern with much lower sidelobes using Dolph-Chebychev amplitude distribution. Table II is the phase and amplitude values in the simulation to achieve Fig. 8. The pattern with dashed line represents the pattern generated with the same amplitude for every antenna element. The pattern formed by the amplitudes based on Dolph-Chebychev distribution is shown as solid line in Fig. 8. The sidelobe of the Dolph-Chebychev distribution pattern is almost 15 dB lower than that created by normalized amplitude.

Fig. 9 is the photo of the proposed phased array for radar receiver. This array is fabricated on a Rogers 4350B board, and the size of the board is about 150mm×150mm. Experiments are being carried out the characterize the performance of the fabricated phased array.

IV. DISCUSSION AND CONCLUSION

In this paper, a 24-GHz phased-array for indoor smart radar is proposed. This array consists of 6 horizontally placed antenna elements. Each antenna element is a vertically placed 5-element series-fed microstrip patch array. Simulation of the 5-element patch array shows it has a -16.4 dB sidelobe level and 22.8° beamwidth on the E-plane. The beam of the system can be continuously steered to different directions on the H-plane through a novel vector control array. Each element of the vector control array can independently adjust the phase and amplitude of the corresponding element in the horizontally placed linear array. The principle of the vector controller is illustrated, and the constant-phase-shift attenuator used in the vector controller is designed and simulated. In addition, by adjusting the phase and amplitude at the same time, this array can realize more complex beam forming, such as achieving a much lower sidelobe. This is very useful for indoor smart radar applications. Because no high-frequency phase shifter is used, the proposed phased-array system based on PIN diodes features a lower cost than conventional solutions.

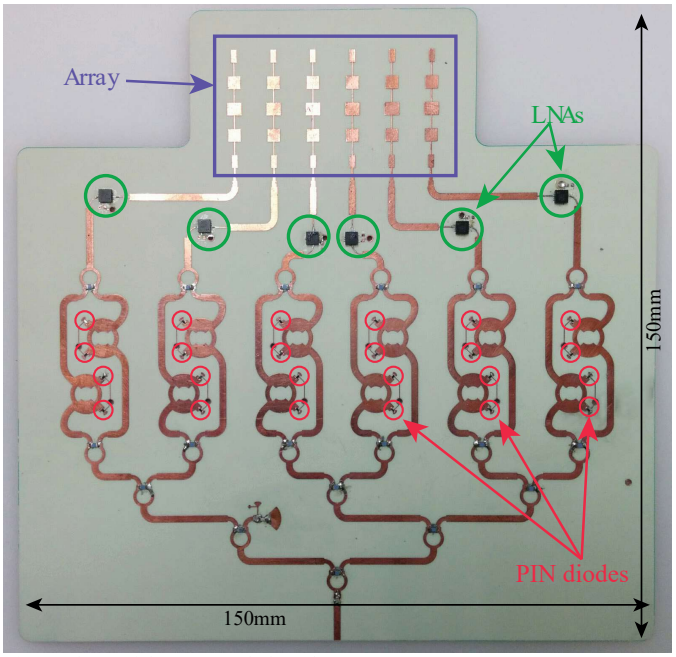

Fig. 9. Photo of the proposed phased-array.

V. ACKNOWLEDGMENT

This work was supported by the National Science Foundation (NSF) under grant ECCS-1254838 and the Cancer Prevention and Research Institute of Texas (CPRIT) under grant RP120053.

REFERENCES

[1] D. M. Grimes and T. O. Jones, "Automotive radar: A brief review," *Proceedings of the IEEE*, vol. 62, no. 6. pp. 804–822, Jun. 1974.

[2] M. Vossiek, L. Wiebking, P. Gulden, J. Wieghardt, C. Hoffmann, and P. Heide, "Wireless local positioning," *Microwave Magazine, IEEE*, vol. 4, no. 4. pp. 77–86, Feb. 2003.

[3] C. Li, V. M. Lubecke, O. Boric-Lubecke, and J. Lin, "A Review on Recent Advances in Doppler Radar Sensors for Noncontact Healthcare Monitoring," *Microwave Theory and Techniques, IEEE Transactions on*, vol. 61, no. 5. pp. 2046–2060, May 2013.

[4] C. Gu, R. Li, H. Zhang, A. Y. C. Fung, C. Torres, S. B. Jiang, and C. Li, "Accurate Respiration Measurement Using DC-Coupled Continuous-Wave Radar Sensor for Motion-Adaptive Cancer Radiotherapy," *Biomedical Engineering, IEEE Transactions on*, vol. 59, no. 11. pp. 3117–3123, Oct. 2012.

[5] H. J. Visser, *Array and Phased Array Antenna Basics*. Chichester, U.K.: Wiley, 2006.

[6] H. L. V. Trees, *Optimum Array Processing*, *1st ed*. New York: Wiley-Interscience, 2002.

[7] W.-T. Kang, I.-S. Chang, and M.-S. Kang, "Reflection-type low-phase-shift attenuator," *Microwave Theory and Techniques, IEEE Transactions on*, vol. 46, no. 7. pp. 1019–1021, Aug. 1998.

[8] S. Walker, "A low phase shift attenuator," *Microwave Theory and Techniques, IEEE Transactions on*, vol. 42, no. 2. pp. 182–185, Feb. 1994.

[9] I. Bahl and P. Bhartia, *Microwave Solid State Circuit Design*. New York: Wiley, 1988, pp. 667–670.